Computers and Concrete, *Vol. 22, No. 1 (2018) 53-62*
DOI: https://doi.org/10.12989/cac.2018.22.1.053

Mesoscale model for cracking of concrete cover induced by reinforcement corrosion

Junyu Chen[a], Weiping Zhang* and Xianglin Gu[b]

Key Laboratory of Performance Evolution and Control for Engineering Structures, Ministry of Education, Tongji University, 1239 Siping Road, Shanghai 200092, PR China

(Received August 11, 2017, Revised March 14, 2018, Accepted April 19, 2018)

Abstract. Cracking of concrete cover induced by reinforcement corrosion is a critical issue for life-cycle design and maintenance of reinforced concrete structures. However, the critical degree of corrosion, based on when the concrete surface cracks, is usually hard to predict accurately due to the heterogeneity inherent in concrete. To investigate the influence of concrete heterogeneity, a modified rigid-body-spring model, which could generate concrete sections with randomly distributed coarse aggregates, has been developed to study the corrosion-induced cracking process of the concrete cover and the corresponding critical degree of corrosion. In this model, concrete is assumed to be a three-phase composite composed of coarse aggregate, mortar and an interfacial transition zone (ITZ), and the uniform corrosion of a steel bar is simulated by applying uniform radial displacement. Once the relationship between radial displacement and degree of corrosion is derived, the critical degree of corrosion can be obtained. The mesoscale model demonstrated its validity as it predicted the critical degree of corrosion and cracking patterns in good agreement with analytical solutions and experimental results. The model demonstrates how the random distribution of coarse aggregate results in a variation of critical degrees of corrosion, which follows a normal distribution. A parametric study was conducted, which indicates that both the mean and variation of critical degree of corrosion increased with the increase of concrete cover thickness, coarse aggregates volume fraction and decrease of coarse aggregate size. In addition, as tensile strength of concrete increased, the average critical degree of corrosion increased while its variation almost remained unchanged.

Keywords: concrete cover cracking; steel corrosion; mesoscale model; random distribution of aggregate; critical degree of corrosion

1. Introduction

Reinforcement corrosion is a primary factor in the structural performance deterioration of reinforced concrete structures (Firouzi and Rahai 2013, Finozzi *et al*. 2015, Safehian and Ramezanianpour 2015). As reinforcement corrosion initiates and propagates, the volumetric expansion of corrosion products gradually exerts internal pressure on the surrounding concrete, causing longitudinal cracking and even spalling of the concrete cover. Thereafter, reinforcement corrosion may be accelerated due to the easier access of aggressive agents.

Considerable research has been undertaken on the cracking process of concrete cover. Andrade *et al.* (1993), Alonso *et al*. (1998) carried out a series of tests to investigate the radial loss of reinforcement that causes the surface cracking of concrete cover. They observed that the critical radial loss of a steel bar increased with the increase of cover thickness and the bar diameter ratio. Oh *et al.* (2009) used strain gauges to monitor the surface cracking of concrete cover, and established an empirical expression to predict the critical corrosion amount. Obvious discreteness can be found among the tested critical corrosion degrees. Considering the concrete around the steel bar to be a thick-walled cylinder subjected to an internal pressure exerted by corrosion products, Bazant (1979) proposed a model to predict the time it takes for concrete to reach a corrosion-induced cracking of concrete cover. Liu and Weyers (1998) developed a model to determine corrosion-induced cracking time based on the critical amount of corrosion products needed to fill the void space around the steel bar and needed to generate sufficient tensile stresses to crack the concrete cover. By combining damage mechanics with elastic mechanics, Zhao *et al.* (2011) developed a model to estimate the critical amount of steel corrosion, which took account of the mechanical properties of both uncracked and cracked concrete, as well as that of corrosion products. Despite their widespread use, these analytical models could not determine the influence of random distribution of coarse aggregates.

Numerical studies have also been conducted to simulate corrosion-induced cracking of concrete cover with finite element methods. In most of these studies, concrete is assumed to be a homogeneous material. Hansen and Saouma (1999) applied uniform radial displacement to

*Corresponding author, Professor
E-mail: weiping_zh@tongji.edu.cn
[a]Ph.D. Student
E-mail: 1410226_chen@tongji.edu.cn
[b]Professor
E-mail: gxl@tongji.edu.cn

http://www.techno-press.org/?journal=cac&subpage=8 ISSN: 1598-8198 (Print), 1598-818X (Online)

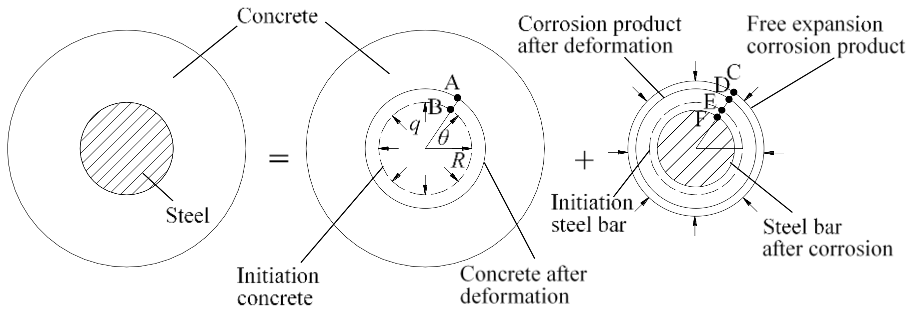

Fig. 1 Deformation of surrounding concrete caused by corrosion expansion of steel bar

simulate the uniform corrosion, and the cracking process of concrete decks was investigated by presetting cracking path in finite element meshes. Jang and Oh (2010) explored the effect of non-uniform corrosion on the cracking behavior of concrete cover and found that cracks in concrete cover caused by expansive pressure under non-uniform corrosion were much smaller than those cracks in cases with uniform corrosion. The discrete element method was used in some simulations, offering a new insight into crack propagation within concrete cover. Tran *et al.* (2011) developed a corrosion-expansion model which was based on a three-dimensional rigid-body-spring (RBSM) method to simulate the crack penetration and failure pattern due to reinforcement corrosion. Grassl and Davies (2011) developed a lattice model to figure out this problem. Richard *et al.* (2016) used the combining discrete element/finite element approach to analyze the local failure mechanisms related to corrosion-induced cracking. On the other hand, more and more researchers have found that the failure behavior of concrete was closely associated with the heterogeneities of the concrete mesostructure (Šavija *et al.* 2013). Du *et al.* (2014) simulated concrete as a composite composed of aggregate, mortar matrix and ITZ, and found that the mesoscale heterogeneous model could reflect the failure pattern of concrete cover more reasonably. However, the influence of coarse aggregates' random distribution on the randomness of critical corrosion degree have not been analyzed in most mesoscale models (Šavija *et al.* 2013, Du *et al.* 2014, Du and Jin 2014, Chen *et al.* 2016). Furthermore, the finite element methods (Hansen and Saouma 1999, Jang and Oh 2010, Du *et al.* 2014, Xi and Yang 2017) were based on continuum mechanics and inherently neglected the conversion from continuous materials to discontinuous materials due to the initiation and propagation of cracks.

In this paper, considering the heterogeneity of concrete, which is mainly caused by the random distribution of coarse aggregate, a modified rigid-body-spring model based on the discrete element method was established to investigate the corrosion-induced cracking process of concrete cover and the corresponding critical degree of corrosion. Concrete is regarded as a three-phase composite composed of coarse aggregate, mortar and an interfacial transition zone (ITZ). The uniform corrosion of steel bar was simulated by applying uniform radial displacement. Finally, a thorough parametric study was conducted to investigate the influences of cover thickness, tensile strength of concrete, volume fraction and size of coarse aggregates on the critical degree of corrosion.

2. Basic assumption for modeling of corrosion cracking process

At the very beginning of a steel bar's corrosion, corrosion products freely expand into the porous transition zone between the steel bar and its surrounding concrete. As corrosion propagates, the corrosion products expand with a volume that exceeds that of their original counterpart by as much as 2 to 6 times (Liu and Weyers 1998). This expansion causes pressure to form on the surrounding concrete. The increased expansive pressure will cause cracking in the surrounding concrete, and finally longitudinal cracking will occur on the surface of the concrete cover.

The critical degree of corrosion when the longitudinal crack occurs on the concrete surface can be approximately the sum of three components (Zhao *et al*. 2011): 1) the corrosion degree η_{pore} for free expansion in the porous transition zone, 2) the corrosion degree η_{stress} causing cracks on the surface of concrete, and 3) the corrosion degree η_{crack} corresponding to the corrosion products penetrating into the corrosion-induced cracks

$$\eta_{\mathrm{s}} = \eta_{\mathrm{pore}} + \eta_{\mathrm{stress}} + \eta_{\mathrm{crack}} \tag{1}$$

The η_{pore} can be established by the method in Zhao *el al.* (2011)

$$\eta_{\mathrm{pore}} = \frac{2Rt_{\mathrm{p}} + t_{\mathrm{p}}^2}{(\alpha - 1)R^2} \tag{2}$$

where R is the initial radius of the steel bar; α is the volumetric ratio of corrosion products to the original steel counterparts and t_{p} is the equivalent thickness of the porous zone around the steel/concrete interface.

The η_{stress} can be calculated by the relationship between the radial displacement of steel/concrete interface and corrosion degree. The deformation of surrounding concrete caused by corrosion expansion is schematically given in Fig. 1. In Fig. 1, q is the expansive pressure; C is the concrete cover thickness; $\delta_{\mathrm{c},\theta}=l_{\mathrm{AB}}=l_{\mathrm{DE}}$ is the radial displacement of the concrete at the interface between the concrete and steel bar; $\delta_{\mathrm{s},\theta}=l_{\mathrm{EF}}$ is the radial loss of the steel bar; $\delta_{\mathrm{fr},\theta}=l_{\mathrm{CF}}$ is the free expansive displacement of corrosion

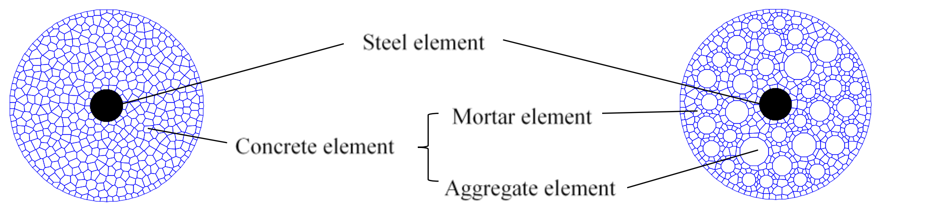

(a) Homogeneous model (b) Heterogeneous model

Fig. 2 Element division of homogeneous model and heterogeneous model

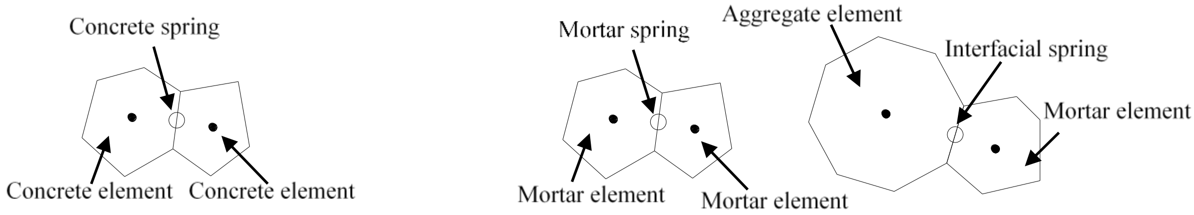

(a) Homogeneous model (b) Heterogeneous model

Fig. 3 Spring connection of homogeneous model and heterogeneous model

products, and $\delta_{r,\theta}=l_{CD}$ is the compressive displacement of corrosion products.

η_{stress} can be obtained from the radial loss of the steel bar

$$\int_0^{2\pi} \delta_{s,\theta} R \mathrm{d}\theta = \eta_{stress}\pi R^2 \tag{3}$$

Assuming that the corrosion product and its expansion ratio α is equal at each point around the steel bar, which means $\delta_{fr,\theta}=\alpha\delta_{s,\theta}$, the deformation compatibility relationship for corrosion products can be expressed as

$$R+\delta_{c,\theta} = R+(\alpha-1)\delta_{s,\theta}-\delta_{r,\theta} \qquad 0<\theta<2\pi \tag{4}$$

with the assumption that the uncorroded steel bar is rigid; then, the compressive displacement of corrosion products $\delta_{r,\theta}$ can be deduced as follows

$$\delta_{r,\theta} = \frac{\alpha(1-v_r^2)R\sqrt{(\alpha-1)\eta_{stress}+1}}{E_r\left\{\left[(1+v_r)\alpha-2\right]+2/\eta_{stress}\right\}}q \tag{5}$$

where E_r and v_r denote the normal elastic modulus and Poisson's ratio of corrosion products, respectively.

For simplicity, five assumptions were made in the mesoscale model for concrete cover cracking. 1) reinforcement corrosion is spatially uniform, and the thickness of corrosion products around reinforcement is identical; 2) the thickness of the porous zone around the steel/concrete interface t_p was taken as 15 μm, which is recommended three-stage model proposed by Liu and Weyers (1998); 3) the volumetric ratio of corrosion products to the original steel counterparts α is assumed to be a constant value, which is equal to 2 as suggested by Zhao *el al.* (2011); 4) the corrosion products are regarded as elastic materials, and E_r=100 MPa, while v_r=0.25 as reported in Zhao *et al.* (2011); 5) the possible penetration of corrosion products into the corrosion-induced cracks (Zhao *et al.* 2013) was not considered in the present study, which means η_{crack}=0. It should be noted that Zhao *et al.* (2016) proposed a two-stage model based on a series of experiments conducted by Chernin *et al.* (2010), Zhao *et al.* (2013), which can better describe the cracking process than Liu and Weyers' model (1998). With the reason that some of the parameters in the two-stage model are difficult to determine, the relatively simple model, three-stage model was adopted in the proposed mesoscale model.

3. Mesoscale model for cracking of concrete cover

A two-dimensional mesoscale model (Wang *et al.* 2008, Gu *et al.* 2013a), which had been successfully used to investigate concrete mechanical properties (Gu *et al.* 2013b), was employed here to simulate the cracking process of the concrete cover. Different from FEM models, the mesoscale model is based on the discrete element method (DEM) by modifying the rigid-body-spring model (Nagai *et al.* 2013).

3.1 Element division and spring connection

Both homogeneous and heterogeneous models were established. The mesoscale model was verified with theoretical analysis by using a homogeneous model; then, the discreteness of concrete cracking is discussed by using the heterogeneous model. In the heterogeneous model, concrete is considered as a three-phase composite composed of coarse aggregate, mortar and ITZ, while there are only concrete elements in the homogeneous model. As shown in Fig. 2, the coarse aggregate elements in the heterogeneous model were treated as regular polygons and randomly distributed into the concrete section. The mortar elements in the heterogeneous model and concrete elements in the homogeneous model were discretized into rigid polygons by using the Voronoi diagram (Gu *et al.* 2013a).

Each element has one rotational and two translational degrees of freedom and connects with its neighboring

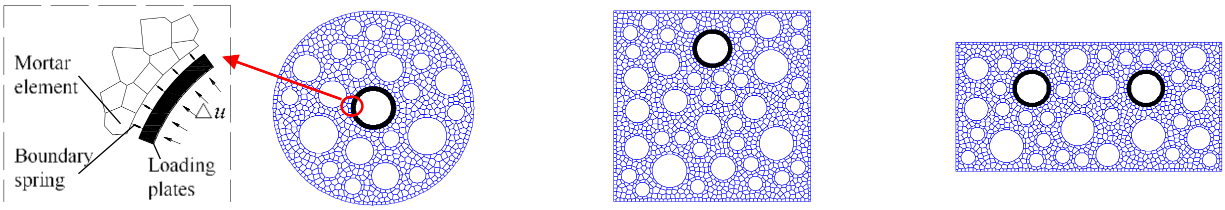

(a) Circular section and loading plate details (b) Square section (c) Adjacent reinforcement

Fig. 4 Loading of model with different sections and adjacent reinforcement

elements by zero-sized springs along their common boundaries. As shown in Fig. 3, the concrete elements connect with one another by concrete springs in the homogeneous model. In the heterogeneous model, the interfacial springs connect both aggregate and mortar elements, and the mortar springs connect two mortar elements. All elements are assumed to be “rigid”, and the deformations of elements are represented by those of springs. The constitutive model of springs and the fracture criterion of springs are based on the experimental results (Gu *et al.* 2013b). To describe the conversion from continuous material to discontinuous material after the spring fails, the connection between the two elements will change to a contact relationship. When the elements contact after the material cracks, the compressive and shear stresses will generate on the common boundaries by contact actions. Instead, when the elements separate, the stresses on the common boundaries will disappear.

3.2 Simulation of corrosion expansion of steel bars

Newton’s equation of motion was applied to each element

$$M\ddot{U}+\alpha M\dot{U}=F \tag{6}$$

The displacements of elements were obtained from the explicit integration of the equation of motion by central finite difference method

$$\dot{U}(t+\Delta t/2)=\frac{\dot{U}(t-\Delta t/2)(1-\alpha\Delta t/2)+\dfrac{F(t)}{M}\Delta t}{1+\alpha\Delta t/2} \tag{7}$$

$$\Delta U=\dot{U}(t+\Delta t/2)\Delta t \tag{8}$$

$$U(t+\Delta t)=U(t)+\Delta U \tag{9}$$

where M, F and U are the generalized mass, resultant force and displacement vectors of an element, respectively; α is the damping coefficient; Δt is the time interval.

The value of α was derived by the critical damping coefficient

$$\alpha=\sqrt{\frac{k_{n,e}}{m_e}} \tag{10}$$

The time interval was given by

$$\Delta t\le T/10=\frac{\pi}{5}\sqrt{m_e/k_{n,e}} \tag{11}$$

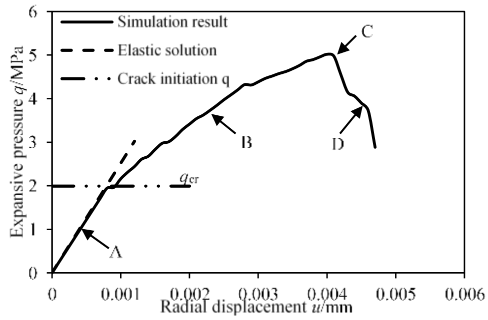

Fig. 5 Relationship between expansive and displacement

where m_e is the mass of the element, $k_{n,e}$, is the normal stiffness of the spring in the proposed model, and T is the natural resonance period of the element. More details about the simulation algorithm were introduced by Gu *et al.* (2013a).

The uniform corrosion of a steel bar was simulated by applying uniform radial displacement, which was achieved by inserting loading plates at the interface between concrete and reinforcement, as shown in Fig. 4(a). It should be noted that the rebar is not shown in Fig. 4 and the loading plates do not exist in the actual situation. Moreover, boundary springs connecting the loading plates and concrete/mortar elements were used to convert the displacement of the loading plate into spring force. The expansive pressure q can be obtained by getting the mean value of the boundary springs force after the deformation of each step. Two different sections of concrete with different positions of steel bars are shown in Fig. 4(b) and Fig. 4(c), respectively.

4. Model verification

4.1 Cracking process of concrete cover

A reinforced concrete cylinder was taken as an example to study the cracking process of concrete cover by using both homogeneous and heterogeneous models. In the model, R=10 mm, C=35 mm, E_c=3.14×10^4 MPa, v_c=0.2, and f_t=2.2 MPa. The simulation result in Fig. 5 was calculated by a homogeneous model and shows the relationship between expansive pressure q and radial displacement u. Fig. 6 shows the crack patterns at key points A, B and C. It should be noted that the red curves on the concrete section represent the break of springs, which means the occurrence of cracks.

As shown in Figs. 5 and 6, the cracking process of concrete cover can be divided into three stages: elastic

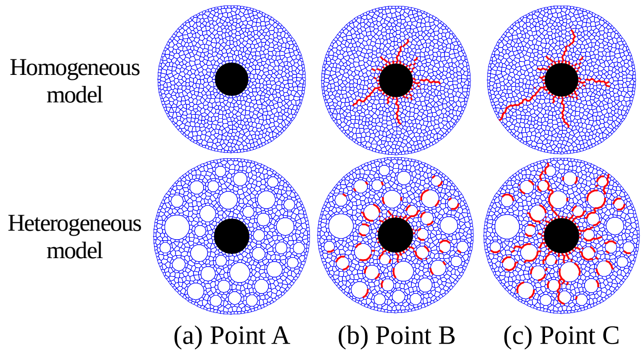

Fig. 6 Crack pattern at key points A, B and C of homogeneous model and heterogeneous model

stage (OA), damage accumulation stage (AC) and unloading stage (CD). In the first stage, no cracks are present in neither the homogeneous nor heterogeneous models, and the mechanical properties of concrete cover remain linear elastic. In the second stage, the stiffness of concrete decreases as cracks appear and propagate. Compared with the homogeneous model, the heterogeneous model can capture the presence of cracks at ITZ between the coarse aggregate and mortar (Point B). Finally, cracks break through the concrete cover, meanwhile, the expansive pressure q reaches the maximum value (Point C). In the third stage, the expansive pressure gradually decrease with the increase of radial displacement.

4.2 Comparison with elastic analytical results before cracks initiation

Concrete cover remains linear elastic before crack initiation at the interface between concrete and reinforcement, so the simulation result in the elastic stage is compared with the elastic analytical solution to validate the model, as shown in Fig. 5. For a thick-walled cylinder under uniform internal pressure q, the circumferential stress σ_θ and radial displacement u at the place with the radial distance from center r can be derived

$$\sigma_\theta = \frac{qR^2(R+C)^2}{C^2+2RC}\cdot\frac{1}{r^2}+\frac{qR^2}{C^2+2RC} \tag{12}$$

$$u = \frac{q}{E}[(1+v)\frac{R^2(R+C)^2}{C^2+2RC}\cdot\frac{1}{r}+(1-v)\frac{R^2}{C^2+2RC}r] \tag{13}$$

In Fig. 5, the relationship between expansive pressure q and displacement u caculated by the homogeneous model show good agreement with the elastic analysis before crack intiation (q_{cr}). Assuming that cracks appear at the interface between concrete and reinforcement when the corresponding circumfacial stress reaches the tensile strength of concrete, the critical expansive pressure q_{cr} can be obtained with Eq. (12), where q_{cr}=1.99 MPa. Fig. 7 shows the simulation result of circumferential stress in concrete cover (R<r<R+C) when $\sigma_{\theta|r=R} < f_t$, also shows good agreement with elastic analytic solution.

4.3 Comparison with damage mechanics-based analytical results after cracks initiation

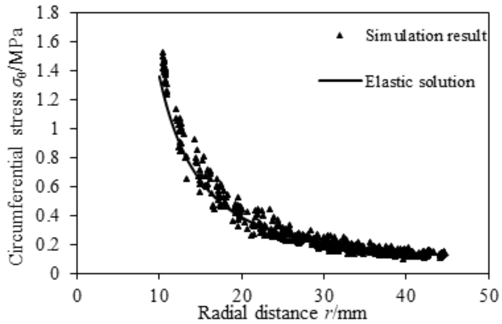

Fig. 7 Circumferential stress in concrete cover (R<r<R+C)

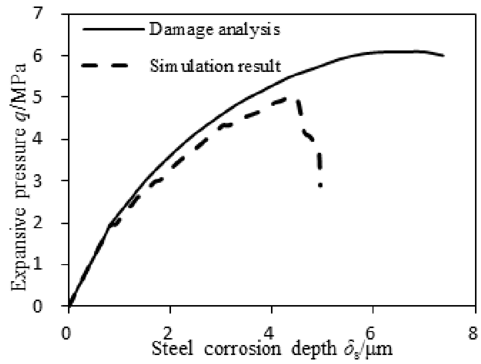

(a) Relationship between expansive pressure and steel corrosion depth

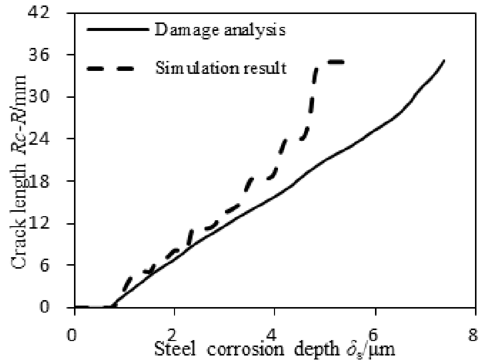

(b) Relationship between crack length and steel corrosion depth

Fig. 8 Comparison between simulation and damage mechanics-based analytical result (Zhao *et al.* 2011)

As cracks further propagate along the radial direction, damage in concrete cover accumulates gradually. Zhao *et al.* (2011) assumed that the concrete cover can be divided into the inner cracked part and the outer intact part. They used elastic mechanics was to analyze the intact part and applied damage mechanics to deal with the cracked part. To verify the applicability of the mesoscale model, a reinforced concrete cylinder example reported by Zhao *et al.* (2011) was set apart to study the development of expansive pressure and propagation of cracks. The values of variables were taken as: R=10 mm, C=35 mm, E_c=3.14×10^4 MPa, v_c=0.2, f_t=2.2 MPa, E_r=100 MPa, v_r=0.25, α=2.

The simulated relationship between expansive pressure and corrosion depth by using homogeneous model shows good agreement with the corresponding damage mechanics-

(a) Experiment result

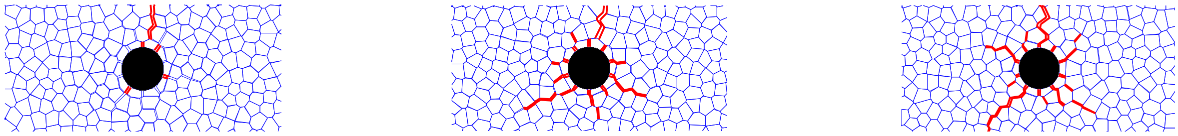

(b) Homogenous simulation

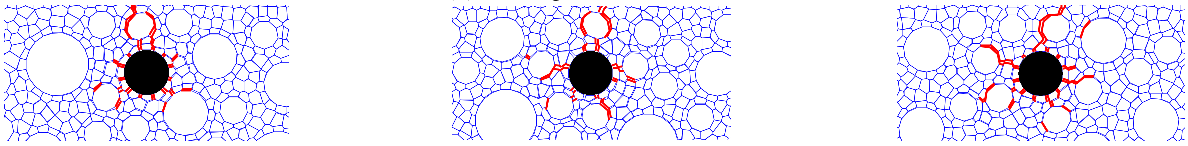

(c) Heterogeneous simulation

Fig. 9 Comparison between experiment (Tran *et al.* 2011) and simulation with side-located reinforcements

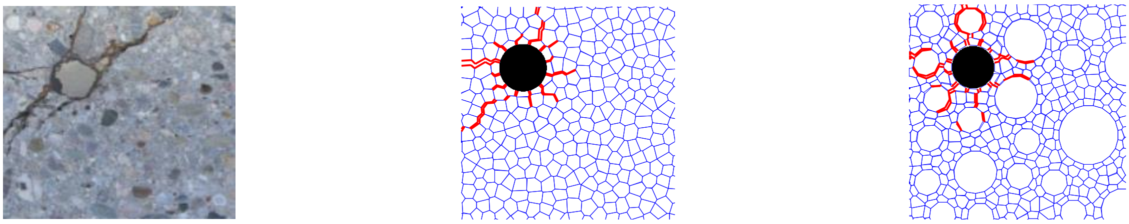

(a) Experiment result (b) Homogenous simulation (c) Heterogeneous simulation

Fig. 10 Comparison between experiment (Fischer 2013) and simulation with corner-located reinforcements

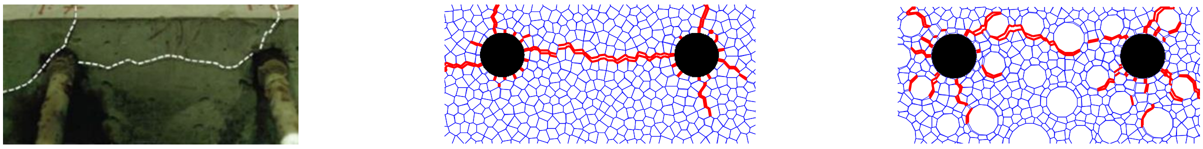

(a) Experiment result (b) Homogenous simulation (c) Heterogeneous simulation

Fig. 11 Comparison between experiment (Vu *et al.* 2005) and simulation with adjacent reinforcements

based analytical results (Zhao *et al.* 2011), as shown in Fig. 8. Cracks occur at the interface between concrete and reinforcement almost with the same corrosion depth in two simulation results (δ_s=0.97 μm). As shown in Fig. 8(a), the maximum value of expansive pressure calculated with the mesoscale model was smaller than the damage mechanics analysis, which was probably due to the brittleness of concrete cover in the mesoscale model. When the expansive pressure reached its maximum value (δ_s=4.32 μm), the crack length rapidly increased from 24 mm to 35 mm in the mesoscale model as shown in Fig. 8(b); thereafter, the first crack appeared on the surface of the concrete cover.

4.4 Verification of cracking pattern

Cracking of concrete cover with different reinforcement positions has been simulated by both a homogeneous model and heterogeneous model. Figs. 9-11 compare cracking patterns between simulation results and available experimental observations (Tran *et al.* 2011, Fischer 2013, Vu *et al.* 2005). The dimensions and material parameters of these collected concrete specimens are summarized in Table 1.

Table 1 Dimensions and material parameters in collected experiments

Experiments	Reinforcement diameter *D*/mm	Concrete cover thickness *C*/mm	Concrete tensile strength f_t/MPa	Concrete elastic modulus *E*/MPa
Tran *et al.* (2011)	19	30	1.53	22500
Fischer (2013)	12	20	3.0	25000
Vu *et al.* (2005)	16	25	3.06	25500

As shown in Figs. 9-11, the cracking patterns obtained by the present mesoscale model were in good agreement with the available experimental observations, demonstrating the reliability and rationality of the present simulation approach. Moreover, compared with the homogeneous model, the cracking patterns calculated by using the heterogeneous model can well describe the tortuosity of cracks propagation due to the random distribution of coarse aggregate. However, with the assumption of uniform corrosion and rounded aggregates, some differences remain

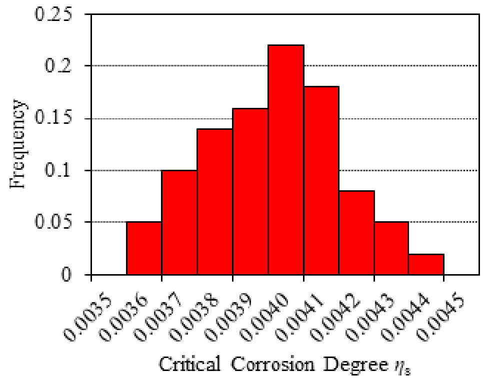

Fig. 12 Probability distribution of critical corrosion degrees

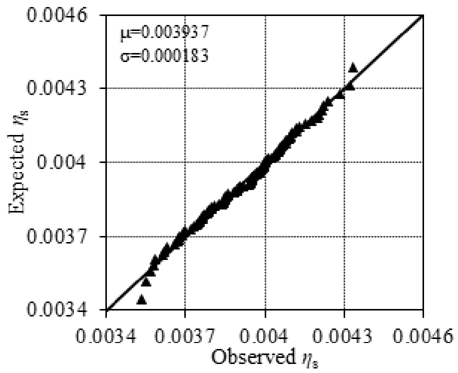

Fig. 13 Normal test on calculated critical corrosion degrees

between simulated cracking patterns and experimentally observed ones.

4.5 Probability distribution of critical degree of corrosion and verification

To investigate the influences of random distribution of coarse aggregates, a concrete cylinder was taken to calculate critical degree of corrosion by using the heterogeneous model. The probability distribution of critical corrosion degree can be obtained by repeating 100 calculations as recommend by Gu *et al.* (2013a) and shown in Fig. 12. In these calculations, R=10 mm, C=35 mm, E_c=29,396 MPa, v_c=0.2, f_t=2.45 MPa. Fig. 13 presents the normal test on the calculated critical corrosion degrees by using Q-Q plot ("*Q*" stands for quantile) (International Organization for Standardization, 1997), which is a graphical method for comparing expected and observed probability distributions by plotting their quantiles against each other. Clearly, the probability distribution of critical corrosion degree can be well described by a normal distribution.

Comparisons between corrosion degree η_s predicted by the mesoscale model and experimental data are summarized in Table 2, where the mean value μ and the standard deviation σ are calculated by the heterogeneous model. Most of the experimental data are between the upper and lower limit values predicted by the proposed model. The predicted mean critical corrosion degrees are generally smaller than experimental ones, probably because corrosion products filling into cracks are neglected in the numerical simulation. On the other hand, non-uniform corrosion was not considered in the mesoscale model. Hence, the predicted critical corrosion degree may have been delayed due to uniform corrosion.

5. Parametric analysis and discussion

5.1 Effect of concrete cover thickness

The thickness of concrete cover ranging from 35 mm to 50 mm was considered in the analysis, while keeping all the other parameters unchanged as reported in Section 4.5. The influences of concrete cover thickness on the mean value and variation of critical corrosion degree are shown in Fig. 14. Clearly, the mean value of critical corrosion degree increases with the increase in concrete cover thickness since the confined effect of concrete cover is enhanced. Moreover, with the increase of concrete cover thickness, the amount of coarse aggregates in the concrete cover increases; then, the complexity of the crack propagation paths increases, which can lead to the increase of variation in the critical corrosion degree.

Table 2 Comparison of corrosion degrees η_s between model predictions and experimental observations

Experiments	Rebar diameter D/mm	Concrete cover thickness C/mm	Concrete tensile strength f_t/MPa	Concrete elastic modulus E/MPa	Corrosion degree η_s			
					Test result	Predicted value		
						Mean value μ	Upper limit μ+3σ	Lower limit μ-3σ
Andrade *et al.* (1993)	16	20	3.55	32000	0.0045	0.00475	0.00516	0.00434
Alonso *et al.* (1998)	16	20	3.55	32000	0.0036	0.00475	0.00516	0.00434
	16	30	3.55	32000	0.0053	0.00526	0.00598	0.00454
Zhang (1999)	16	25	1.54	25500	0.0043	0.00448	0.00478	0.00419
	20	25	1.54	25500	0.0039	0.00356	0.00379	0.00332
	25	25	1.54	25500	0.0030	0.00284	0.00308	0.00261
	16	30	1.54	25500	0.0058	0.00467	0.00510	0.00424
	16	35	1.54	25500	0.0062	0.00485	0.00554	0.00415
Vidal *et al.* (2004)	12	16	4.7	32000	0.0067	0.00609	0.00664	0.00554
	6	16	4.7	32000	0.0199	0.01278	0.01484	0.01072

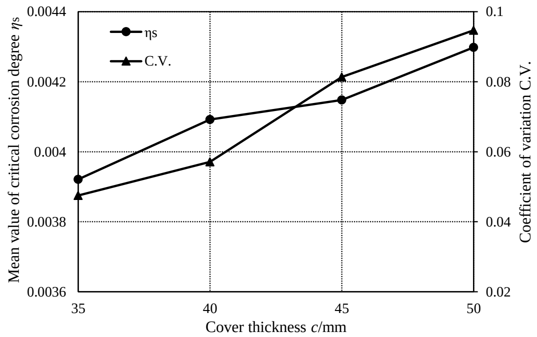

Fig. 14 Effect of concrete cover thickness on the mean value and variation of critical corrosion degree

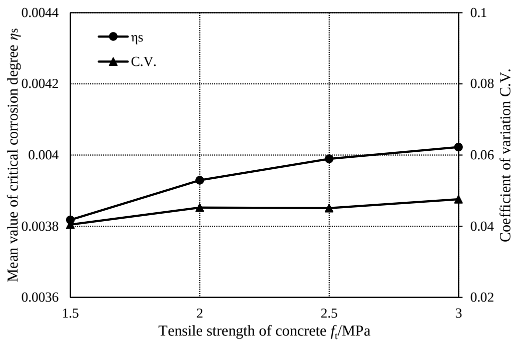

Fig. 15 Effect of concrete tensile strength on the mean value and variation of critical corrosion degree

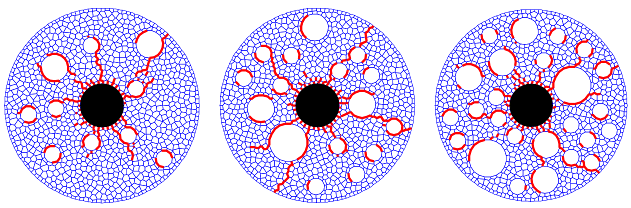

(a) V_f=0.2 (b) V_f=0.4 (c) V_f=0.6

Fig. 16 Modeling the random distribution of aggregate with various aggregate volume fractions

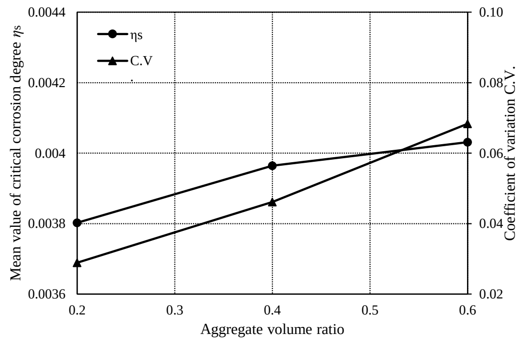

Fig. 17 Effect of coarse aggregate volume fraction on the mean value and variation of critical corrosion degree

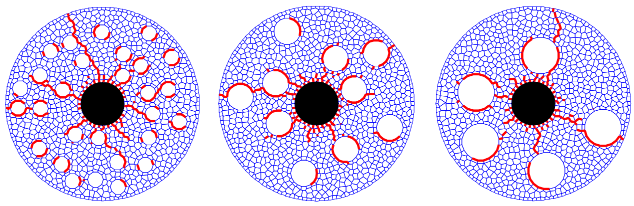

(a) D_{agg}=7 mm (b) D_{agg}=12 mm (c) D_{agg}=17mm

Fig. 18 Modeling the random distribution of aggregate with different coarse aggregate size

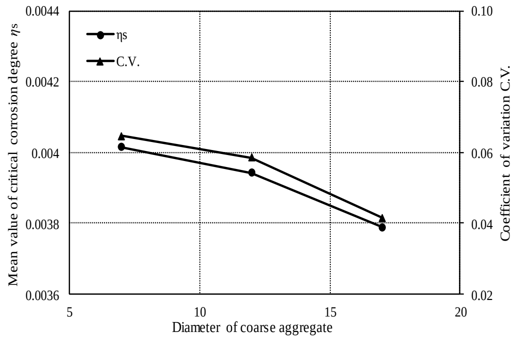

Fig. 19 Effect of relatively small aggregate volume ratio on the mean value and variation of critical corrosion degree

5.2 Effect of concrete tensile strength

The influences of concrete tensile strength on the mean value and variation of critical corrosion degree are graphed in Fig. 15, which shows how as the tensile strength increases, the mean value of critical corrosion degree also increase as expected. However, since the concrete section size and coarse aggregate volume fraction remain unchanged in the analysis, the complexity of crack penetration paths caused by random distribution of coarse aggregate almost remains the same. Therefore, no obvious influence of concrete tensile strength on the variation of critical corrosion degree was found in Fig. 15.

5.3 Effect of coarse aggregate volume fraction

For specimens with different coarse aggregate volume fraction, corrosion-induced cover cracking patterns when the first crack occurs on the surface are compared in Fig. 16. The influences of coarse aggregate volume fraction on the mean value and variation of critical corrosion degree are shown in Fig. 17. As the coarse aggregate volume fraction increases, the length of weak ITZ between aggregate and mortar is on the rise; however, the number of coarse aggregate, which is regarded as a rigid body in the present model, also increases, eventually resulting in the increased mean value of critical corrosion degree. Meanwhile, the variation of critical corrosion degree increases as the complexity of crack penetration paths increases.

5.4 Effect of coarse aggregate size

A single particle size distribution is adopted and the diameters of coarse aggregate range from 7 mm to 17 mm, while keeping the volume fraction of coarse aggregate unchanged. For specimens with different coarse aggregate size, corrosion-induced cover cracking patterns when the first crack occurs on the surface are compared in Fig. 18. The influences of coarse aggregate size on the mean value and variation of critical corrosion degree are shown in Fig.

19. With the increasing size of coarse aggregate, the mean value of critical corrosion degree decreases because longer weak surfaces (ITZ) exist in larger aggregate. Moreover, since the crack penetration path is relatively simple, the variation of critical corrosion degree also decreases.

6. Conclusions

Considering the concrete heterogeneities caused by random distribution of coarse aggregates and assuming the uniform corrosion-induced expansion, the cracking behavior of concrete cover induced by reinforcement corrosion was thoroughly studied with a mesoscale model. The proposed model was verified by a wide range of experimental observations and results. Thereafter, parametric study was conducted to investigate the influences of cover thickness, tensile strength of concrete, volume fraction and size of coarse aggregates on the statistical characteristics of critical corrosion degree. Based on the scope of this paper, several conclusions can be drawn:

- Compared with damage analysis, the brittleness of concrete cover cracking is more obvious in the proposed mesoscale model. Once the expansive pressure reached the maximum value, the cracks penetrated through the concrete cover rapidly. It seems to be more reasonable for quasi-brittle materials such as concrete, more validation should be conducted in the future research.
- Considering the random distribution of coarse aggregates, the crack propagation paths may be tortuous and various since the cracks usually pass through the surface of coarse aggregate. Thereafter, this study showed that the critical degree of corrosion is a random variable, and it fits the normal distribution well.
- The parametric study indicated that both the mean and variation of critical corrosion degree increase with the increase of concrete cover thickness, the coarse aggregate volume fraction and the decrease of coarse aggregate size. As concrete tensile strength increases, the average critical degree of corrosion increases while its variation remains almost unchanged.

Acknowledgments

This research project was financially supported by the National Key Basic Research Program of China (973 Program, No. 2015CB655103) and National Natural Science Foundation of China (Grant No. 51578402).

References

Alonso, C., Andrade, C., Rodriguez, J. and Diez, J.M. (1998), "Factors controlling cracking of concrete affected by reinforcement corrosion", *Mater. Struct.*, **31**(7), 435-441.

Andrade, C., Alonso, C. and Molina, F.J. (1993), "Cover cracking as a function of bar corrosion: Part I-Experimental test", *Mater. Struct.*, **26**(8), 453-464.

Bazant, Z.P. (1979), "Physical model for steel corrosion in concrete sea structures-theory", *J. Struct. Div.*, **105**(ST6), 1137-1153.

Chen, A., Pan, Z. and Ma, R. (2016), "Mesoscopic simulation of steel rebar corrosion process in concrete and its damage to concrete cover", *Struct. Infrastr. Eng.*, **13**(4), 478-493.

Chernin, L., Val, D. and Volokh, K. (2010), "Analytical modelling of concrete cover cracking caused by corrosion of reinforcement", *Mater. Struct.*, **43**(4), 543-556.

Du, X. and Jin, L. (2014), "Meso-scale numerical investigation on cracking of cover concrete induced by corrosion of reinforcing steel", *Eng. Fail. Anal.*, **39**, 21-33.

Du, X., Jin, L. and Zhang, R. (2014), "Modeling the cracking of cover concrete due to non-uniform corrosion of reinforcement", *Corros. Sci.*, **89**, 189-202.

Finozzi, I., Berto, L. and Saetta, A. (2015), "Structural response of corroded RC beams: a comprehensive damage approach", *Comput. Concrete*, **15**(3), 411-436.

Firouzi, A. and Rahai, A. (2013), "Reliability assessment of concrete bridges subject to corrosion-induced cracks during life cycle using artificial neural networks", *Comput. Concrete*, **12**(1), 91-107.

Fischer, C. (2013), "Beitrag zu den Auswirkungen der Bewehrungsstahlkorrosion auf den Verbund zwischen Stahl und Beton", Ph.D. Dissertation, Stuttgart University, Stuttgart. (in Germany)

Grassl, P. and Davies, T. (2011), "Lattice modelling of corrosion induced cracking and bond in reinforced concrete", *Cement Concrete Compos.*, **33**(9), 918-924.

Gu, X., Hong, L., Wang, Z. and Lin, F. (2013), "A modified rigid-body-spring concrete model for prediction of initial defects and aggregates distribution effect on behavior of concrete", *Comput. Mater. Sci.*, **77**, 355-365.

Gu, X., Hong, L., Wang, Z. and Lin, F. (2013), "Experimental study and application of mechanical properties for the interface between cobblestone aggregate and mortar in concrete", *Constr. Build. Mater.*, **46**, 156-166.

Hansen, E.J. and Saouma, V.E. (1999), "Numerical simulation of reinforced concrete deterioration: Part II - Steel corrosion and concrete cracking", *ACI Mater. J.*, **96**(3), 331-340.

International Organization for Standardization (ISO) (1997), Statistical Interpretation of Data-Tests for Departure from the Normal Distribution.

Jang, B.S. and Oh, B.H. (2010), "Effects of non-uniform corrosion on the cracking and service life of reinforced concrete structures", *Cement Concrete Res.*, **40**(9), 1441-1450.

Liu, Y.P. and Weyers, R.E. (1998), "Modeling the time-to-corrosion cracking in chloride contaminated reinforced concrete structures", *ACI Mater. J.*, **95**(6), 675-680.

Nagai, K., Sato, Y. and Ueda, T. (2004), "Mesoscopic simulation of failure of mortar and concrete by 2D RBSM", *J. Adv. Concrete Technol.*, **2**(3), 359-374.

Oh, B.H., Kim, K.H. and Jang, B.S. (2009), "Critical corrosion amount to cause cracking of reinforced concrete structures", *ACI Mater. J.*, **106**(4), 333-339.

Richard, B., Quiertant, M., Bouteiller, V., Delaplace, A., Adelaide, L., Ragueneau, F. and Cremona, C. (2016), "Experiment and numerical analysis of corrosion-induced cover cracking in reinforced concrete sample", *Comput. Concrete*, **18**(3), 421-439.

Safehian, M. and Ramezanianpour, A. (2015), "Prediction of RC structure service life from field long term chloride diffusion", *Comput. Concrete*, **15**(4), 589-606.

Šavija, B., Luković, M., Pacheco, J. and Schlangen, E. (2013), "Cracking of the concrete cover due to reinforcement corrosion: A two-dimensional lattice model study", *Constr. Build. Mater.*, **44**, 626-638.

Tran, K.K., Nakamura, H., Kawamura, K. and Kunieda, M.

(2011), “Analysis of crack propagation due to rebar corrosion using RBSM”, *Cement Concrete Compos.*, **33**(9), 906-917.
Vidal, T., Castel, A. and François, R. (2004), “Analyzing crack width to predict corrosion in reinforced concrete”, *Cement Concrete Res.*, **34**(1), 165-174.
Vu, K., Stewart, M.G. and Mullard, J. (2005), “Corrosion-induced cracking: Experimental data and predictive models”, *ACI Struct. J.*, **102**(5), 719-726.
Wang, Z., Lin, F. and Gu, X. (2008), “Numerical simulation of failure process of concrete under compression based on mesoscopic discrete element model”, *Tsinghua Sci. Technol.*, **13**(S1), 19-25.
Xi, X. and Yang, S.T. (2017), “Time to surface cracking and crack width of reinforced concrete structures under corrosion of multiple rebars”, *Constr. Build. Mater.*, **155**, 114-125.
Zhang, W.P. (1999), “Damage prediction and durability estimation for corrosion of reinforcement in concrete structures”, Ph.D. Dissertation, Tongji University, Shanghai. (in Chinese)
Zhao, Y., Dong, J. and Jin, W. (2016), “Corrosion-induced concrete cracking model considering corrosion product-filled paste at the concrete/steel interface”, *Constr. Build. Mater.*, **116**, 273-280.
Zhao, Y., Wu, Y. and Jin, W. (2013), “Distribution of millscale on corroded steel bars and penetration of steel corrosion products in concrete”, *Corros. Sci.*, **66**, 160-168.
Zhao, Y., Yu, J. and Jin, W. (2011), “Damage analysis and cracking model of reinforced concrete structures with rebar corrosion”, *Corros. Sci.*, **53**(10), 3388-3397.

HK